

# Nanosized Iron Oxide Particles Entrapped in Pseudo-Single Crystals of $\gamma$ -Cyclodextrin

Daniele Bonacchi,<sup>†</sup> Andrea Caneschi,<sup>†</sup> Dominique Dornigac,<sup>‡</sup> Andrea Falqui,<sup>§</sup>  
Dante Gatteschi,<sup>\*,†</sup> Donella Rovai,<sup>†</sup> Claudio Sangregorio,<sup>†</sup> and Roberta Sessoli<sup>†</sup>

UdR INSTM, Dipartimento di Chimica, Università di Firenze, Sesto Fiorentino,  
FI, I-50019, Italy, CEMES–CNRS, 29 Rue Jeanne Marvig, 31055 Toulouse, France, and  
Dipartimento di Scienza Chimica, Università di Cagliari,  
Cittadella Universitaria di Monserrato, I-09042, CA, Italy

Received October 2, 2003. Revised Manuscript Received December 22, 2003

A new technique to produce very small magnetic nanoparticles of maghemite ( $\gamma$ -Fe<sub>2</sub>O<sub>3</sub>) is presented. The particles form and precipitate in the presence of the oligosaccharide  $\gamma$ -cyclodextrin and in the final product remain entrapped in tiny pseudo-single crystals of the organic host. Evidence of nanosized particles embedded in the organic crystal was obtained by HR-TEM studies that showed the occurrence of uniformly dispersed particles with average diameter of 18 Å. The resulting objects gave diffraction patterns with the same spacing as that of cyclodextrin crystals without iron. The magnetic properties were investigated by ZFC–FC magnetizations, hysteresis loops, and ac susceptibility measurements. The compound presents a complex magnetic behavior that deviates from that predicted on the basis of the classic single domain particle model. The deviation is ascribed to the complex properties of the surface, which, for such small sizes, plays the major role in determining the total magnetic behavior.

## Introduction

The search for new synthetic strategies for the fabrication of magnetic particles with nanometer-scale size is currently a challenging research area.<sup>1</sup> The basic requirement that a technique must satisfy in order to allow the design of new nanostructured materials is the control over the particle sizes and, possibly on their assembly. Embedding techniques, such as those that use reverse micelles, ion-exchange resins, and zeolites or the sol–gel approach, offer the possibility to tune the particle size in a wide range but, in most cases, at the expense of their homogeneity.<sup>2</sup> On the other hand, molecular techniques have provided spectacular results both in terms of new magnetic properties and of structural features.<sup>3</sup> The advantage of the molecular approach is that of giving rise to absolutely monodisperse objects, regularly arranged in a lattice, whose structure can be

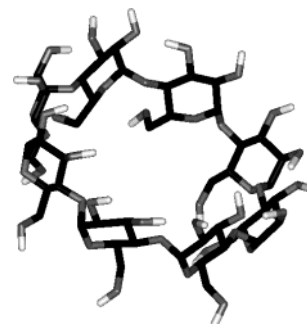


**Figure 1.** Structure of  $\gamma$ -cyclodextrin ( $\gamma$ -CD); the hydrogen atoms bound to carbons are not shown for clarity.

perfectly known through X-ray crystal analysis and whose properties can be determined with great accuracy. The main disadvantage of this approach is that so far it has not been possible to increase the size of the particles beyond the limit of a few hundred atoms. In the case of magnetic systems, it has not been possible to grow molecules containing more than 30 centers.<sup>4</sup>

The use of cyclodextrins as ligands to form polynuclear complexes of magnetic metal ions has not been fully exploited. Cyclodextrins are a family of well-known, natural, cyclic oligosaccharides that are torus-like macrorings built up from six ( $\alpha$ -cyclodextrin), seven ( $\beta$ -cyclodextrin), or eight ( $\gamma$ -cyclodextrin) glucopyranose units. A schematic view of the structure of  $\gamma$ -cyclodextrin, ( $\gamma$ -CD) is sketched in Figure 1. Cyclodextrin can be easily deprotonated and in this form is able to complex with different metal ions. The main interest

\* Corresponding author. E-mail: dante.gatteschi@unifi.it.

<sup>†</sup> Università di Firenze.

<sup>‡</sup> CEMES–CNRS.

<sup>§</sup> Università di Cagliari.

(1) O'Connor, C. J.; Tang, J.; Zhang, J. H. in *Magnetism: Molecules to Materials III*; Nanosized Magnetic Materials; Miller, J. S., Drillon, M., Eds.; Wiley-VCH: Weinheim, 2001; p 1.

(2) (a) Pillai, V.; Kumar, P.; Hou, M. J.; Ayyub, P.; Shah, D. O. *Adv. Colloid Interface Sci.* **1995**, *55*, 241. (b) Moumen, N.; Pileni, M. P. *Chem. Mater.* **1996**, *8*, 1128. (c) Pileni, M. P.; Moumen, N.; Lisiecki, I.; Bonville, P.; Veillet, P. *Nanoparticles in Solids and Solutions*; Fendler, J. H., Dekany, I., Eds.; Kluwer Academic Publisher: Netherlands, 1996; p 325. (d) Ziolo, R. F.; Giannelis, E. P.; Weinstein, B. A.; O'Horo, M. P.; Ganguly, B. N.; Mehrotra, V.; Russel, M. W.; Huffman, D. R. *Science* **1992**, *257*, 219. (e) Abe, T.; Tachibana, Y.; Uematsu, M.; Iwamoto, M. *J. Chem. Soc. Chem. Commun.* **1995**, *16*, 1617. (f) Brinker, C. J.; Scherer, G. W. *Sol–Gel Science*; Academic Press: New York, 1990.

(3) (a) Gatteschi, D.; Caneschi, A.; Pardi, L.; Sessoli, R. *Science* **1994**, *265*, 1054. (b) Sessoli, R.; Gatteschi, D.; Caneschi, A.; Novak, M. A. *Nature* **1993**, *365*, 141.

(4) (a) Muller, A. et al. *Angew. Chem., Int. Ed. Engl.* **1999**, *38*, 3238. (b) Soler, M.; Rumberger, E.; Foltz, K.; Hendrickson, D. N.; Christou, G. *Polyhedron* **2001**, *20*, 1365.

in using cyclodextrins as ligands is that they offer a rich and complex chemistry and also that they are nontoxic and hence suitable for medical application.<sup>5</sup>

In an attempt to synthesize polynuclear magnetic metal ion compounds with structure similar to those reported for lead and other nonmagnetic ions,<sup>6,7</sup> we have now found that small particles of iron oxide, presumably of maghemite ( $\gamma\text{-Fe}_2\text{O}_3$ ), with very small average diameter (1.8 nm) and with a narrow size distribution can be entrapped in pseudo-single crystals of  $\gamma\text{-CD}$ . In this paper, we wish to report the results of the analysis of the structural and magnetic properties of this new type of particle embedding technique and wish to discuss its general relevance.

### Experimental Section

Single crystals of the compound  $\gamma\text{-Fe}_2\text{O}_3/\gamma\text{-CD}$  (**1**) were prepared as follows: ferrous chloride was added to a solution obtained dissolving  $\gamma\text{-CD}$  in DMF and the solution was stirred under Ar for 2 h. An ethanolic solution of NaOH was then added and the resulting solution was kept stirring for 0.5 h and then air-exposed. Cubic-shaped orange-reddish single crystals separated out after few weeks from the filtered solution under ethanol diffusion. The ligand:metal ion:base ratio was 1:8:8. Elemental analysis for **1** gave C, 33.6; H, 5.37; N, 0.24; Fe, 8.4.

Nondoped crystals of  $\gamma\text{-CD}$  were prepared by following the same procedure but replacing the iron chloride with NaCl and adjusting the pH value to that of the corresponding iron-containing solution.

XRD patterns were collected at 100 K on a CCD-1K Bruker diffractometer. The XRD patterns reported in this paper were taken with a Laue Camera working at ambient temperature while a Bruker D8 Advance instrument was used for powder XRD spectra.

TEM images were obtained with a Philips CM30 TEM operating at 300 kV with point resolution 2.0 Å. Micrographs were taken on a slice of a few nanometers thick obtained by grinding a single crystal.

Mössbauer spectra were recorded with a home-built instrument operating with a [ $^{57}\text{Co}$  in Rh] source; a Gifford-Mac Mahon cryogenerator was used to cool the sample.

Magnetic measurements were performed using a Cryogenic S600 SQUID magnetometer and a VSM from Oxford Instruments. Single-crystal magnetic measurements were performed with a home-built microsquid at the L. Néel-CNRS in Grenoble, France.

### Results and Discussion

Single crystals of **1** were obtained by addition of a base to a  $\text{FeCl}_2$  solution in the presence of  $\gamma\text{-CD}$ . After the addition of the base under inert atmosphere, a white precipitate forms. When the product is exposed to oxygen, it turns to green and then slowly dissolves in the solution, changing its color to red-brown. This observation is in good agreement with the formation of magnetite and then subsequent oxidation to maghemite from Fe(II) hydroxide via the so-called green-rust, a Fe(II)–Fe(III) hydroxy salt.<sup>8</sup> Probably it is at this stage that the cyclodextrin limits the growth of the iron oxide crystallites interacting with the surface of the small particles. The metal content of the dried compound,

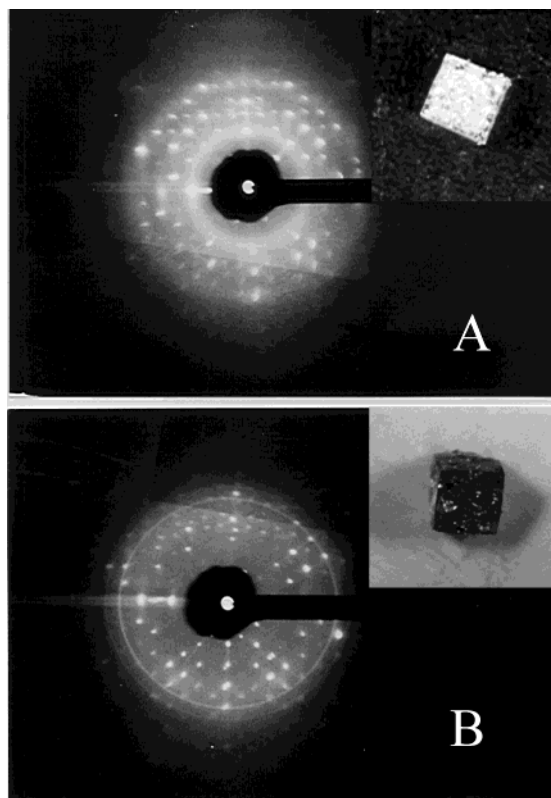


**Figure 2.** X-ray diffraction patterns of pure  $\gamma\text{-CD}$  (A) and of iron oxide  $\gamma\text{-CD}$  (B); the two patterns have the same spacing. Images of the crystals are shown in the insets.

evaluated from elemental analysis, was 8.4% and, assuming that all iron is present as  $\text{Fe}_2\text{O}_3$  (see below), approximately corresponds to 20 iron ions for 9  $\gamma\text{-CD}$  molecules.

Crystals were orange-reddish and cubic-shaped and gave diffraction patterns that looked like those of a single crystal (Figure 2). From the full diffraction data set collected at 100 K, we determined a cubic unit cell with a 30.217 Å edge. The symmetry and systematic absences of the reciprocal lattice were consistent with the space group  $I432$ , a space group that has never been observed for  $\gamma\text{-CD}$  nor for any of its complexes. Unfortunately, the maximum resolution limit was very low (reflections were observed only to a resolution  $\lambda/2 \sin \theta = 1.4$  Å), and that prevented the structure determination by direct methods. The poor diffraction crystal quality can be ascribed either to the large amount of disordered solvent molecules entrapped in the crystals, as already observed in other  $\gamma\text{-CD}$  complexes,<sup>9,10</sup> or to the presence of large disordered aggregates of iron ions. The presence of a large amount of solvent was confirmed by elemental analysis, which indicated the presence of several molecules of DMF, and by the crystals' sensitivity to air exposure (once crystals are removed from mother liquor they crack within few seconds, probably due to the loss of ethanol molecules).

Since we found that it is possible to obtain seemingly similar pseudo-crystals in a range of iron from 0 to 10% we studied also crystals containing  $\gamma\text{-CD}$  only. These crystals were prepared following the same procedure

(5) Fromming, K.; Szejtli, J. *Cyclodextrins in Pharmacy*; Kluwer Academic Publisher: Dordrecht, 1994.

(6) Klüfers, P.; Schuhmacher, J. *Angew. Chem., Int. Ed. Engl.* **1994**, *33*, 1863.

(7) Fuchs, R.; Habermann, N.; Klüfers, P. *Angew. Chem., Int. Ed. Engl.* **1993**, *32*, 852.

(8) Cornell, R. M.; Schwertmann, U. *The Iron Oxides*; VCH: Weinheim, 1996.

(9) Steiner, T.; Saenger, W. *Acta Crystallogr.* **1998**, *B54*, 450.

(10) Kamitori, S.; Hirotsu, K.; Higuchi, T. *Bull. Chem. Soc. Jpn.* **1988**, *61*, 3825.

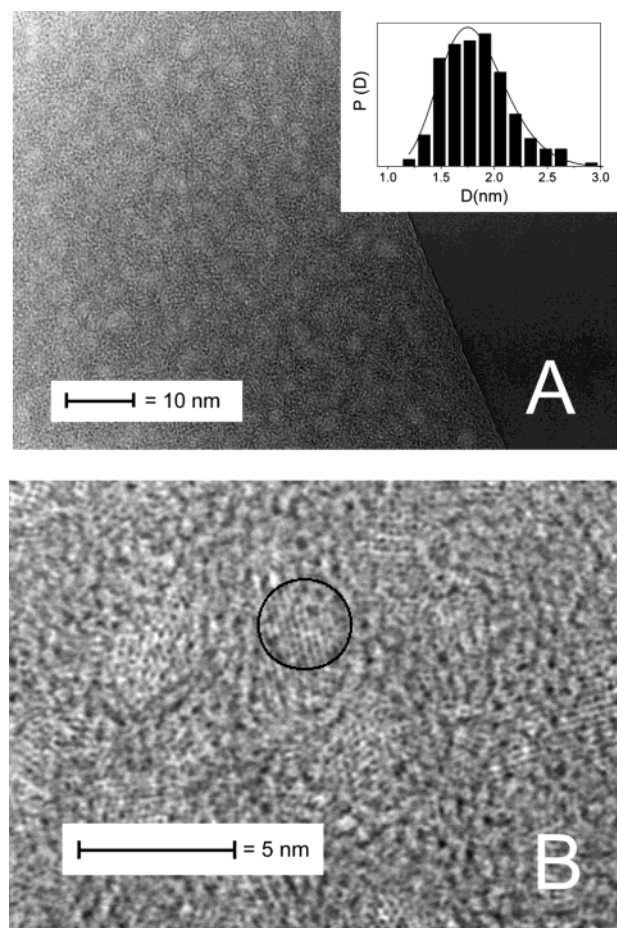


**Figure 3.** HREM micrographs showing the occurrence of a uniform distribution of almost identical, well-separated nanoparticles (A) and the crystalline order of each particle (B). The size distribution obtained from a statistic over 210 particles is shown in the inset.

used for **1**. The colorless cubic crystals gave diffraction patterns similar to those of **1** from which the same cubic unit cell was determined. Unfortunately also the poor quality of the crystals was similar (the observed reflections were less than 10% for  $d < 1.2$  Å) making all the attempts to solve the structure either by direct methods or by molecular replacement, unsuccessfully. Beside the low crystallinity, the difficulties met in solving the structure may also arise from twinning or to an extended polycrystallinity of the material.

Evidence of the presence of nanoparticles in crystals of **1** was obtained from high resolution-TEM (HREM) images (Figure 3a). Micrographs show a uniform distribution of nanoparticles inside the organic matrix. The size distribution, obtained from a statistic over 210 nanoparticles, is narrow and could be well-reproduced by a log-normal distribution with average diameter of 18 Å and  $\sigma = 0.19$ . The HREM images show clearly that inside the bigger particles a crystalline order is present (Figure 3b), and comparison of the 2-D projection of the nanoparticle crystal structure observed in the images with the HREM-simulated images of many iron oxides and hydroxides structures allows us to identify the nanophase as the maghemite phase ( $\gamma$ -Fe<sub>2</sub>O<sub>3</sub>), although we cannot exclude that the crystalline order is absent in the smaller particles. The particles appear well-separated from each other, even if the images do not allow us to draw any conclusion concerning the 3D

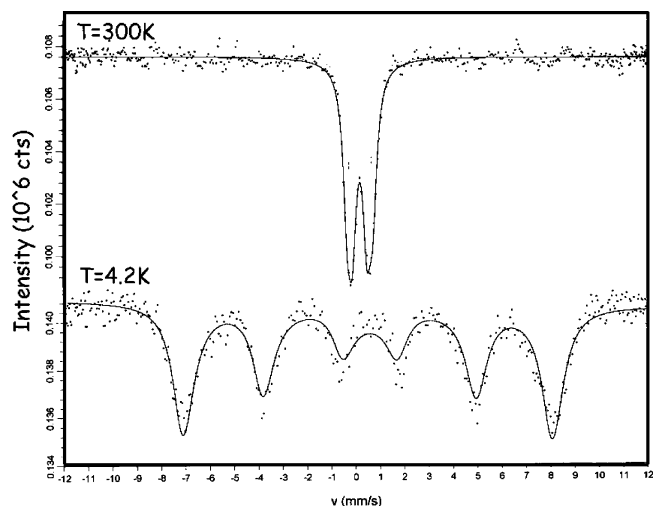


**Figure 4.** Mössbauer spectra recorded at room (top curve) and liquid helium temperature (bottom curve); the doublet observed at room temperature splits in to a sextet below the blocking temperature.

**Table 1. Mössbauer Parameters for **1** and for Bulk Maghemite (Taken from ref 8)**

oxide	temp (K)	isomer shift (mm s <sup>-1</sup> )	quadrupole splitting (mm s <sup>-1</sup> )	hyperfine field (T)
Fe <sub>2</sub> O <sub>3</sub> /γ-CD ( <b>1</b> )	4.2	0.50	0	47.2
maghemite	4.2	0.48	0	51.7

arrangement. From the average diameter estimated from TEM analysis and assuming that inside each particle the iron oxide has the same crystal structure of bulk maghemite, we can evaluate that, on average, each particle comprises ca. 110 iron ions. Combining these data with elemental analysis we can roughly estimate that there is about one particle per four unit cells (the same estimate can be obtained from the experimental densities of the iron-doped and nondoped crystals, 1.57 and 1.43 g·cm<sup>-3</sup>, respectively).

Powder X-ray diffraction spectra, as expected, did not show any peaks relative to the inorganic phase, due to the small size of the particles.

The Mössbauer spectra evolve from a doublet at ambient temperature to a single sextet at 4.2 K (Figure 4), confirming the presence of only trivalent iron; isomer shifts, quadrupole splittings, and hyperfine fields values are in good agreement with those reported for maghemite, as shown in Table 1. The temperature evolution of the spectra confirms the presence of single domain magnetic particles: at room temperature, when the relaxation time of the particle's magnetic moments,  $\tau$ , is shorter than the measuring time,  $\tau_{\text{exp}}$ , a paramagnetic spectrum is observed, while at the liquid helium temperature, where  $\tau$  is longer than  $\tau_{\text{exp}}$ , the spectrum looks like that of bulk maghemite.

The observation of the same space group,  $I432$ , and unit cell parameters of the doped and nondoped crystals seems to indicate that the entrapment of iron oxide particles does not disturb the crystalline packing of  $\gamma$ -CD molecules.  $\gamma$ -CD is well-known to form several stable inclusion complexes hosting organic molecules in the hydrophobic cavity,<sup>11</sup> but the cavity sizes are not large enough to host particles as large as those observed with HREM. Larger cavities, however, could be gener-



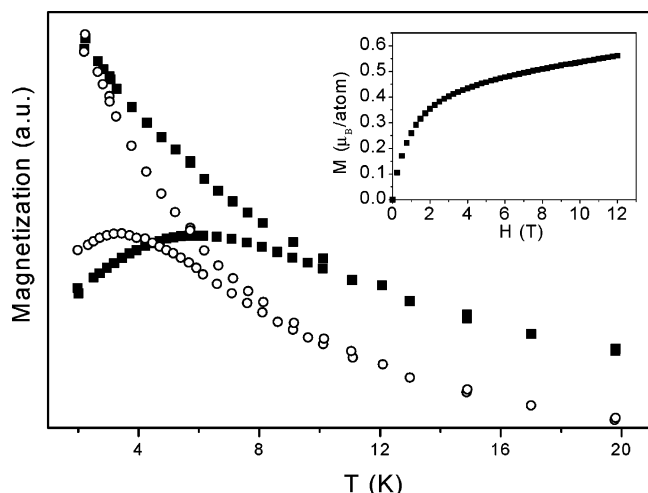


**Figure 5.** Normalized ZFC and FC magnetizations of the crystals (■) and of the DMF solution (○) measured with an applied field of 5 mT. In the inset the  $M$  vs  $H$  curve of the powder measured at 1.5 K is shown.

ated by the molecular packing. Several compounds containing  $\gamma$ -CD have been reported in the literature and all of them crystallize only in two different space groups: the hydrate compounds crystallize in the monoclinic  $P2_1$  space group,<sup>12</sup> while all the complexes are packed in the tetragonal  $P4_22$  space group.<sup>9,10,13</sup> To our knowledge, no cubic space groups have ever been observed. Thus, none of the previously reported structures can be taken as a model for the crystalline packing, and no conclusions can be drawn whether large voids, normally filled by solvent molecules, are formed or not. Alternatively, it can be guessed that particles are randomly enclosed in the growing crystal, partially replacing part of the many solvent molecules present and creating defects that do not significantly affect the crystal packing of the organic molecules.

The magnetic properties of **1** agree with those expected for an assembly of randomly oriented single domain particles. The temperature dependence of the zero field cooled and field cooled magnetizations, measured with an applied field of 5 mT, is shown in Figure 5. This irreversibility is often attributed to the characteristic blocking–unblocking process of the particle magnetic moment when thermal energy is varied; as the relaxation time of a magnetic particle increases with decreasing temperature, we can define, for a certain observation time, a characteristic average temperature, called blocking temperature, below which the particle moment appears blocked on the time scale of the experiment. In the case of DC magnetization measurements, the blocking temperature is usually assumed to coincide with the temperature of the maximum of the ZFC curve,  $T_{\max}$ . In our case, the ZFC magnetization exhibits a maximum at 5.8 K, indicating that particles are characterized by a small average energy barrier. The

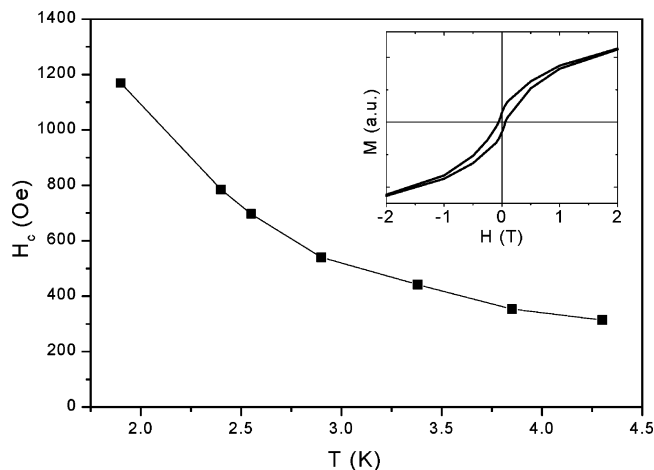


**Figure 6.** Temperature dependence of the coercive field. The line is a guide to the eyes. The inset shows the hysteresis loop at 1.9 K.

small separation between  $T_{\max}$  and the temperature at which the ZFC and FC curves split is instead an indication of a narrow energy barrier distribution.

However, it cannot be excluded that what we observe is a spin-glass-like behavior, due to strong interparticle interactions or to disorder present in the material itself. In fact, in both cases the same thermal irreversibility in the magnetization is expected. Supporting this last thesis, the  $M$  vs  $H$  curve at 1.5 K, shown in the inset of Figure 5, does not reach saturation up to the largest measuring field of 12 T. Such behavior reflects the occurrence of spin canting and/or of a large disordered spin surface, as should be expected for particles a few nanometers in diameter. In fact, in such particles most metal ions lie on the surface where they have a reduced coordination, which can favor spin configurations different from the fully aligned one, introducing the disorder and frustration needed for spin-glass behavior. To have a rough evaluation of the strength of the dipolar interaction, a simple calculation using the point dipole approximation,<sup>14</sup> the average values of the particles magnetic moment evaluated from the high-temperature magnetic susceptibility, and the estimated average interparticle distance (50 Å) has been performed. The obtained value is less than 200 mK, much lower than 6 K, ruling out the possibility that the observed behavior in the ZFC curve is due to magnetic ordering, as indeed confirmed by other experimental results (see below).

Hysteresis loops open below  $T_{\max}$  with a large coercivity, if compared to usual maghemite nanoparticles of comparable size.<sup>15</sup> The coercive field increases on decreasing temperature, reaching ca. 120 mT at 1.9 K, as shown in Figure 6. Hysteresis loops of a single crystal of **1** were also measured at low temperature with a microSQUID along the three principal crystal axes. No differences were observed, indicating a random distribution of the easy axis of the nanoparticles inside the pseudo-single crystal.

To investigate in more detail the nature of the irreversibility observed in the ZFC–FC curve, we measured the temperature dependence of the ac susceptibility at dif-

(11) Harata, K. *Chem. Rev.* **1998**, *98*, 1803.

(12) (a) Harata, K. *Bull. Chem. Soc. Jpn.* **1987**, *60*, 2763. (b) Hingerty, B. E.; Betzel, C.; Saenger, W. *Am. Cryst. Assoc., Abstr. Papers* **1984**, *12*, 37.

(13) (a) Kamitori, S.; Hirotsu, K.; Higuchi, T. *J. Chem. Soc. Chem. Commun.* **1986**, *113*, 690. (b) Kamitori, S.; Hirotsu, K.; Higuchi, T. *J. Am. Chem. Soc.* **1987**, *109*, 2409. (c) Ding, J.; Steiner, T.; Zabel, V.; Hingerty, B. E.; Mason, S. A.; Saenger, W. *J. Am. Chem. Soc.* **1991**, *113*, 8081.

(14) Morrish, A. H. *The Physical Principles of Magnetism*; John Wiley & Sons: New York, 1966.

(15) Leslie-Pelecky, D. L.; Rieke, R. D. *Chem. Mater.* **1996**, *8*, 1770–1783.

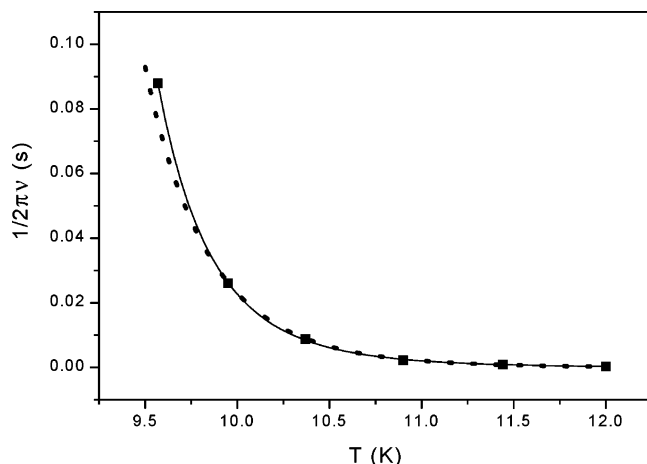


**Figure 7.** Relaxation time as a function of temperature obtained from the maxima of the in-phase component of the ac susceptibility. The two lines represent the fitting with a power law (full line) and the Arrhenius law (dot line).

ferent frequencies. When the interactions between particles can be ignored, the frequency dependence of the maximum of the susceptibility can be interpreted with a thermal activated model, developed in the 1940s by Néel,<sup>16</sup> which predicts that the temperature dependence of the relaxation time,  $\tau$ , should follow an Arrhenius law:

$$\tau = \tau_0 \exp(\Delta E/k_B T)$$

where  $\Delta E$  is the average energy barrier and is given by  $\Delta E = KV$  ( $K$  being the anisotropy energy constant and  $V$  the particles volume) and  $\tau_0$  is a time constant that is usually on the order of  $10^{-9}$ – $10^{-11}$  s. The fit of our data to this model, shown in Figure 7, gives for the average energy barrier  $KV/k_B = 265$  K and a low value of  $\tau_0 = 7 \times 10^{-15}$  s, which is closer to what is commonly observed for spin-glass systems rather than for nanoparticles.<sup>17</sup> Furthermore, from the average particles  $\Delta E$  value and using the average particles volume obtained from HREM measurement, we evaluated the anisotropy constant  $K$ , which being independent from the particle volume is more representative of the material.  $K$  is equal to  $1.2 \times 10^6$  J/m<sup>3</sup>, at least 1 order of magnitude larger if compared to larger maghemite nanoparticles ( $K = 10^4$ – $10^5$  J/m<sup>3</sup>). Such discrepancies are often taken as an indication that interparticle interactions strongly influence the dynamics of reorientation of the magnetization.<sup>17</sup> However, due to the small size of the particles and hence to the particularly relevant role of the surface, as recent studies suggest,<sup>19</sup> it is more probable that what we observe is the result of the glasslike behavior of the single particle. Finally, we wish to point out that for our system the frequency dependence of the maximum of the ac susceptibility could be satisfactorily reproduced using a power law  $\tau = \tau_0 [T_g/(T - T_g)]^z$  with  $T_g$  as the glass temperature and  $z$  as the critical

exponent, which is commonly used in spin-glass systems.<sup>18</sup> The best fit parameters obtained in this case were  $T_g = 7.6 \pm 0.2$  K,  $\tau_0 = (8.2 \pm 0.5) \times 10^{-6}$ , and  $z = 6.8 \pm 0.8$  (Figure 7); the  $T_g$  value is larger than the observed blocking temperature, an anomalous behavior which is still under investigation, while the  $z$  value is in good agreement with what is commonly observed for strongly interacting nanoparticle systems.<sup>20</sup>

Crystals of **1** are highly soluble in DMF, DMSO, and water. The solutions obtained are stable over long periods. The ZFC–FC magnetizations of these solutions differ from that of the corresponding solid only for a small shift of  $T_{\max}$  to lower temperature (Figure 5), suggesting that stable dispersions of the nanoparticles were attained. The shift of  $T_{\max}$  can be presumably ascribed to a decrease of interparticle interactions.<sup>17</sup> We wish to stress that the magnetic thermal irreversibility observed in the solution is a further confirmation of the effective presence of small nanoparticles in the synthesized objects.

By dissolving **1** in water, an acidic solution is obtained, suggesting that hydrolysis takes place on the particle surface, giving rise to a charged layer responsible of the stable dispersion in water in a range of pH between 2.5 and 5 (the same decrease is not observed in the pure  $\gamma$ -CD); at higher pH values a hydroxide-like substance precipitates.

## Conclusion

In the present study a new technique to prepare very small metal oxide nanoparticles is presented. Once formed particles are entrapped in pseudo-single crystals of  $\gamma$ -CD. The way in which the entrapping process occurs remains obscure. Possibly particles are hosted in large voids generated in the crystal packing or they are randomly enclosed as disordered defects, but in any case their enclosure does not seem to significantly affect the packing mode of  $\gamma$ -CD.

The reduced sizes of the particles and their relatively narrow size distribution make this system an exciting challenge from a scientific point of view, since it lies at the borderline between clusters and “classical” nanoparticles, showing magnetic properties almost unusual and representing an important piece in the knowledge of magnetism. The magnetic behavior of such small particles is far from being totally explained, as it is strongly complicated by the large importance of surface effects. The presence of interparticle interactions further complicates the interpretation.

From a technological point of view, the biocompatibility and solubility of cyclodextrin make this compound suitable for medical application, since they can be used as contrast agent for nuclear magnetic resonance and also as iron delivery carrier in the human body.

**Acknowledgment.** The authors thank Dr. S. Ciatini for technical assistance with XRD data collection, Prof. G. Spina and Dr. F. Del Giallo for Mössbauer measurements, Dr. W. Wernsdorfer of the LCM-CNRS, Grenoble (France) for microSQUID measurements, and C. de Julian for helpful discussion. This work was financially supported by the MIUR and CNR.

CM034948E

(16) Néel, L. *Ann. Geophys.* **1949**, 60, 661.

(17) (a) Dormann, J. L.; Bessais, L.; Fiorani, D. *J. Phys. C* **1988**, 21, 1215. (b) Luo, W.; Nagel, S. R.; Rosenbaum, T. F.; Rosenweig, R. E. *Phys. Rev. Lett.* **1991**, 67, 2721. (c) Djurberg, C.; Svedlindh, P.; Nordblad, P.; Hansen, M. F.; Bødker, F.; Mørup, S. *Phys. Rev. Lett.* **1997**, 79, 5154. (d) Dormann, J. L.; et al. *J. Magn. Magn. Mater.* **1998**, 187, L139. (e) Tronc, E.; et al. *J. Magn. Magn. Mater.* **2000**, 221, 63.

(18) Mydosh, J. A. *Spin Glasses: An Experimental Introduction*; Taylor & Francis Ltd.: London, 1993.

(19) Tronc, E.; et al. *J. Magn. Magn. Mater.* **2003**, 262, 6–14.

(20) Dormann, J. L.; Spinu, L.; Tronc, E.; Jolivet, J. P.; Lucari, F.; D’Orazio, F.; Fiorani, D. *J. Magn. Magn. Mater.* **1998**, 183, L255.